Energy & Buildings 260 (2022) 111850

Contents lists available at ScienceDirect

Energy & Buildings

journal homepage: www.elsevier.com/locate/enb

Optimisation of a recirculating domestic hot water system to minimise wait time and heat loss

R.W. Moss *, R.E. Critoph

School of Engineering, University of Warwick, Coventry CV4 7AL, UK

ARTICLE INFO

Article history:
Received 11 May 2021
Revised 8 January 2022
Accepted 10 January 2022
Available online 15 January 2022

Keywords:
Insulation
Advection
Method of lines
Recirculation
Thermosyphon

ABSTRACT

Many houses suffer from a delay in hot water arrival, after opening the hot tap, due to the length of pipe work from the boiler or thermal store. Measurements in three properties showed delays of up to 46 s. A recirculation system could maintain the water in the pipe at a suitable temperature and for a 15 m pipe is expected to use 30 W less electrical power than a local thermal store at the delivery point. Time-steady eigenvector solutions to the linked temperature equations allow optimisation of the recirculation flow rate, pipe diameters and insulation thickness. The pumping power is <1 mW and a pumpless thermosyphon system should be possible in some installations. Heat loss coefficients have been calculated for a pair of pipes in a common insulation sleeve to minimise the losses. A plug flow transient advection model for water and pipe temperature based on a sliding 1-D grid has been developed and validated for a single pipe, then extended to also model recirculating systems. Heat losses in a pumped system may be reduced using a timer so the system can cool overnight. The transient model predicts the relationship between flow and warm-up rate to optimise pump size and timing.

1. Introduction

1.1. Background

The mean energy consumption by UK houses includes 4 kWh/-day to produce hot water [6]. Improved insulation standards in new houses can reduce the heating load to such an extent that the hot water load approaches 50% of the total heat demand [23]. Measures to improve the efficiency of hot water use by minimising heat losses can therefore make a significant contribution to reducing household energy consumption.

Whilst most houses in the UK currently use 'combi' boilers burning natural gas, the UK government's commitment to reducing carbon emissions mandates an end to fossil-fuel heating installations in new houses from 2025 [20]. It seems likely that the majority of these new houses will use a heat pump, given the scarcity of heating networks in the UK. Carbon-neutral heating targets cannot however be achieved by new-build heat pumps alone. Sugden [32] shows that across the EU, heat pumps need to replace existing fossil fuel boilers at an installation rate of 3 million per annum, compared to the current 500,000 for new build housing, if combustion boilers are to be eliminated by 2050; boosting the public perception of heat pumps is a useful step towards this goal.

There are many disincentives that currently limit the rate of heat pump retrofitting into the existing housing stock. Conversely the installation of a heat pump could provide the initiative to remedy long-standing problems with existing systems. One such problem is the need to run considerable volumes of water through a hot tap before it reaches the desired temperature: this issue has been identified as a major consumer satisfaction metric, Wendt [37], so a solution might help to boost heat pump uptake rates.

1.2. Introduction to hot water delivery systems

Thermal insulation is necessary to minimise the heat loss rates from the hot water pipes during the flow period and after delivery ceases; many older houses however still have uninsulated pipework [37]. The Energy Saving Trust report that 'For summer months, the regular boilers were efficient for generating DHW to the cylinder (average heat efficiency 81%) but recorded heat delivered to taps was much lower. The average efficiency of heat delivered to the taps is only 38%, and much lower where little DHW is used (range 13% to 65%)' [15]. The design of tank heating controls is one approach for increasing the efficiency of hot water systems [22] by reducing heat losses from the tank. The present work, by contrast, aims to reduce heat loss from the pipework whilst simultaneously reducing the wait time.

Each delivery of hot water results in heat wastage as the hot water within the pipe cools down prior to the next tap opening;

* Corresponding author.
E-mail address: r.moss@warwick.ac.uk (R.W. Moss).

https://doi.org/10.1016/j.enbuild.2022.111850
0378-7788/

Nomenclature

c	specific heat capacity J/kgK
c_w, c_p, c_{wp}	heat capacity of water, pipe or water & pipe per metre (J/mK)
$\dot{c}_w$	heat capacity rate of water flow $=\dot{m}c$ (W/K)
h	linear heat transfer coefficient (W/mK), water to pipe
x	distance along pipe (m)
h_{10}, h_{20}, h_{12}	conductances between pipes 1 & 2 or to ambient "0" (W/mK).
h_{ext}	insulation external heat transfer coefficient (W/m^{2}K)
$\boldsymbol{g}$	acceleration due to gravity, 9.81 m/s^2 (scalar and vector)
k	thermal conductivity (W/mK)
$\dot{m}$	mass flow rate (kg/s)
r	radius (m)
t	time since start of flow (seconds).
u	unit step function
d	diameter (m)
H	linear overall heat transfer coefficient, pipe to air (W/mK)
L	pipe length (m)
$\dot{Q}$	heat flux rate (W)
T	temperature (°C)
T_0	pipe temperature at $t = 0$
T_∞	air temperature
ΔT	temperature difference (°C)
U	wall heat loss coefficient (W/m^{2}K)
α	thermal diffusivity (m^2/s)
ε	Effectiveness
θ_1, θ_2	flow and return water temperatures (°C)
μ	dynamic viscosity (Pa.s)
ρ	density (kg/m^3)
τ	time constant (seconds)
Nu	Nusselt number
Pr	Prandtl number
Re	Reynolds number
NTU	Number of Thermal Units

Sub and superscripts

i	Insulation
P_{PP}	pipe
w	water
‘	parameter interpolated between grids

with lengthy pipes there is an associated delay when opening a tap before the water runs hot. This is commonly accepted in older houses with long pipe runs: delays of over 40 s were observed during testing. Minimising this side-effect by updating pipework during a heat pump conversion could be one way of improving customer satisfaction. Haines [17] investigated the role of user satisfaction in terms of hot water provision and concluded that fast-response availability of hot water was essential if users were not to be dissatisfied, given the cost of the conversion itself. Gu [16], Gabrielaitiene [13] and van der Heijde [33] have examined the delay in hot water arrival after the start of flow; the present work builds on this with an improved model that includes the water to pipe heat transfer coefficient and uses a convecting grid to avoid the numerical smearing at the hot/cold interface seen in previously reported work.

Warm water has the potential to harbour *Legionella* bacteria. Bower [5] mentions the advantages of continual water flow in hindering the build-up of bacteria as well maintaining temperatures sufficient to kill *Legionella*. Bedard [11] studied *Legionella pneumophila* adaptation to copper and temperature in a hospital and found bacteria that had adapted to survive at 55 °C. Such matters are a concern for designers but beyond the scope of the present work.

The rate of cooling once a hot tap is closed is related to the quantity of pipe insulation used. Kaynakli [21] reviews optimisation methods for pipe insulation based on economic criteria and fuel prices. Increasing the insulation thickness will reduce the heat loss rate but cool-down time constants for any practical thickness are insufficient to maintain the pipe temperature over periods of an hour or more between water withdrawals.

One promising technique to avoid the delay in hot water arrival is to use a recirculation system that keeps the pipework warm at all times. Such systems are already found in commercial premises and large apartment blocks but have yet to penetrate the household hot water market.

Kitzberger [23] compared the performance of recirculating and instantaneous local heaters for delivering instant hot water in the context of university research buildings and found the delivery efficiency for centralised hot water systems could be 12% or less for low to medium consumption. NREL [26] simulated domestic hot water use in TRNSYS. They identified on-demand heaters as a way of reducing pipework heat losses, giving energy savings of 550 kWh per annum if replacing a high temperature tank and quantified the energy use for a variety of installation options. Similarly Benakopoulos [2] describes recirculation systems for apartment blocks in Denmark and Poland with circulation heat losses of up to 70%. A well-insulated system is therefore essential. For zero consumption the delivery efficiency would inevitably be zero so the present paper discusses the performance in terms of heat loss rate rather than efficiency.

A number of authors have investigated recirculation systems, albeit in non-domestic contexts. Van der Heijde [34] made a thorough study of the steady-state heat loss from equal-diameter recirculating pipes in the context of continuously-flowing district heating networks.

Eatherton [8] describes typical pumped recirculation systems in hotels and apartment complexes: hydraulic erosion corrosion can be a problem unless the system is carefully balanced to avoid excessive water velocities. Eatherton [9] describes the use of Thermal Flow Control valves to automatically balance such pumped systems. Building codes in Wisconsin mandate the use of a recirculating system or electrical heating tape where the source to appliance distance exceeds 30 m [12]. Hamburg [18] measured heat losses from DHW circulation pipes in multi-occupant apartment blocks and correlated their data against pipe length and floor area.

Other authors have studied heat loss rates for conventional DHW systems. Marini [24] produced a Matlab model for calculating hot water heat losses based on flow and duration measurements from 15 houses in the UK, with pipe runs from 5 m up to 20 m. 80% of the heat loss occurred during non-flow periods while pipes cooled down after water use and they estimated that insulating the pipework would reduce losses by 45%. Similarly Bertrand [3] characterised hot water use for 14,000 households in Esch-sur-Alzette using GIS mapping data and assumed distributions for the number of showers, baths and dishwashers.

Wendt [37] created a LabView model to simulate hot water distribution systems in Californian houses. They distinguished between clustered withdrawals, where users withdraw hot water in unison and cold start cases where pipes had time to cool down between one withdrawal and the next. Both continuous and timed

recirculation systems were considered as a way of reducing the wait time, which was measured for 7 houses. A survey of plumbing contractors identified the wait for hot water as a slightly more important measure than initial cost, reliability or flow rate: it is therefore worth designing systems to minimise the wait time, provided this can be done without significantly increased heat losses.

Recirculation systems created without detailed modelling tend to use over-sized pumps [9–12]. This is wasteful of electricity; the electrical power dissipation will contribute to maintaining the water temperature but is an inefficient form of heating compared to a heat pump.

If using a recirculating system for hot water delivery, as opposed to space heating, the return pipe can usefully be made smaller than the delivery pipe. The concept was proposed in a district heating context by Averfalk [10] who calculated heat losses and pumping power using a reduced diameter return pipe.

There is a need for simulation tools that can accurately model the heat transfer between the forward and returning flows such that the required recirculation flow rate can be determined. Conventional 2D and 3D CFD codes such as Fluent and Star-CCM + would require large grids to accurately model the flow and heat transfer within long, small bore pipes and generating a large number of solutions with different pipe sizes and insulation parameters would be a very slow optimisation process. Heat transfer within pipes is however well modelled by simple Nusselt number correlations and a detailed Navier-Stokes solution as used in CFD codes is unnecessary in the context of a domestic heating system design.

Faster simulations would be possible using commercial 1D pipe flow software such as the Pipe Flow Module in COMSOL, Siemens Flomaster or Schlumberger Software's OLGA. Not having access to such specialised software, in the present work the authors decided to use the equation-solving functions in Matlab® to implement a simple solver for transient heat transfer between surroundings and a constant flow rate advecting flow. Matlab is widely used for engineering modelling, with over 4 million users, and the language is particularly suitable for running a large number of simulations to identify the optimum configuration. The resulting code is freely available on the Warwick Research Archive and includes both a steady-state solution and a more detailed transient solver. The latter is not available in prior literature and allows determination of the optimum pipe diameter ratio, insulation distribution and initial warm-up time for intermittently pumped recirculation.

Typical hot water and ambient temperatures of 60 °C and 20 °C have been used for all calculations and graphs, together with a pipe length of 15 m. This is purely to simplify interpretation: actual values will of course vary seasonally and from house to house.

2. Illustration of the problem: experimental determination of hot water time delay

Before examining the theory of advecting flows it may be useful to consider the scale of the problem. Measurements of transit time were taken in three houses with thermal stores and long pipe runs to demonstrate typical delay times (Fig. 1, Table 1).

The test houses were:

(a) House 1 (Oxfordshire): a 3-storey, 3 bedroom end-terrace built in 1993. The gas boiler heats a Range Flowmax vented thermal storage tank in the airing cupboard: this is a combination tank with a built-in header on top. Cold water passes through a finned pipe coil within this tank, generating hot water instantaneously whenever a hot tap is opened. Pipes (uninsulated) pass under the floorboards for the upper floor and then down behind plasterboard wall coverings to the kitchen. The walls have a narrow cavity (of order 8 mm) between the outer reconstituted stone wall (Bekstone®)

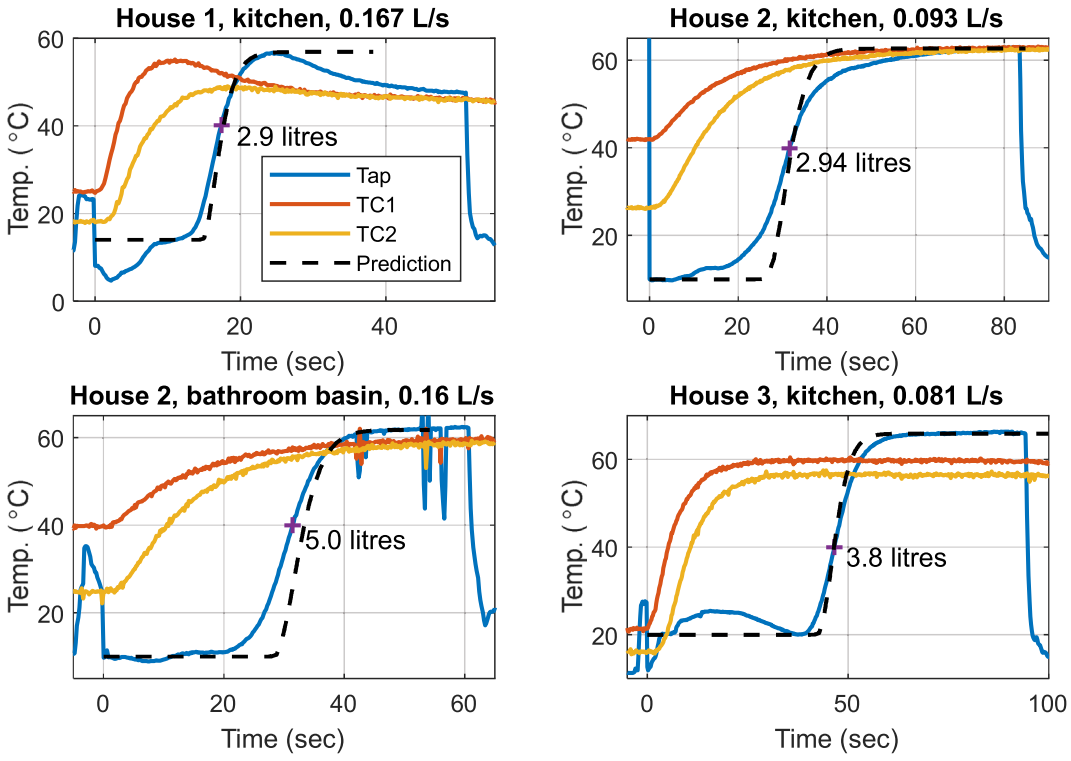

Fig. 1. Examples of hot water arrival times. TC1 and TC2 were close to the hot tank; the final thermocouple was held in the hot stream from the tap. House 1 has a thermostatic valve at outlet from the tank. The prediction (Method of Lines) is described in section 4.3 below.

Table 1
Pipe lengths and thermocouple positions in instrumented houses. The relative lengths of pipe diameters in houses 1 and 3 (†) are estimated values.

House:	1	2	2	3
Pipe to:	Kitchen	Kitchen	Bathroom basin	Kitchen
Pipe length × OD (m)	4 × 0.022, 8.79 × 015†	2.8 × 0.022, 12.95 × 0.015	12.34 × 0.022, 5.0 × 0.015	0.4 × 0.022, 15.16 × 0.015†
Tank to TC1 (m)	0.49	0.5	0.5	0.66
Tank to TC2 (m)	1.0	0.72	0.72	1.3
TC2 to tap (m)	11.3	14.53	16.12	13.6
Pipe volume (L)	2.6†	2.8	4.8	2.3†
Pipe losses heat house?	Y	Y	N	Y

and an aerated concrete inner wall (Thermalite®): the house is poorly insulated by modern standards, $U_{wall} \approx 0.66$ W/m^{2}K.

(b) House 2 (Warwickshire): a 4 bedroom bungalow built in 1958. The construction is cavity walls using concrete and breeze blocks and it has a MegaFlo hot water cylinder heated by an oil-fired Worcester-Bosch boiler. For experimental purposes, however, the tank was heated using an electrical immersion heater. The pipes run though a shallow loft space and are insulated with ClimaFlex® foam.

(c) House 3 (Gloucestershire): a 3-storey, 5 bedroom Cotswold stone house built in 1869. A conventional vented hot water cylinder is heated by an oil-fired Potterton Statesman boiler; there is a header tank in the loft. Pipes are uninsulated and run underneath the first floor floorboards.

Each test was performed early in the morning before any hot water had been used. Data logging was performed using a Measurement Computing HS-1616 USB logger sampling at 5 Hz. Data acquisition started with the tap closed and the tap thermocouple taped in position just below the spout. A hot air gun was used to warm the thermocouple in this position; when the flow started and the thermocouple was surrounded by water, the sudden drop in temperature was then evident in the data. Two more thermocouples (TC1, TC2) were positioned close to the hot tank, taped onto the pipe, to show the initial temperatures here; there was no access to allow measurements further downstream.

The flow was allowed to continue until temperatures had reached steady state, at which point the tap was closed. The flow rate was determined from the volume collected during the flow period; all testing was with the taps fully open. The airing cupboard pipes in house 3 were uninsulated and surface temperatures at positions TC1 & 2 were significantly cooler than the water leaving the kitchen tap.

The predictions in Fig. 1 were obtained via a Method of Lines algorithm (Section 4.3 below). The initial temperature profile along the pipe at $t = 0$ could not be measured because the pipes passed under floorboards and through cavities; the solutions therefore commenced with a uniform pipe temperature and a step in water inlet temperature. The prediction includes heat transfer from water to pipe. The measured exit temperature generally rises more slowly than predicted: this will be partly due to the velocity profile across the pipe mixing hot and cold water [7] and partly due to convection-induced warm water in the pipes near the tank before the flow started.

The hot water cylinder in houses 1 and 3 was located upstairs and the delivery pipes ran downwards so there was no tendency for free convection between tank and pipework. These houses showed a more sudden arrival of hot water at the tap than house 2 which had the initial 2.5 m of pipework running upwards from the tank exit port (0.5 m horizontal, 0.8 m vertical, 1.2 m slanting). The presence of warm water in the house 2 pipework is indicated by the initial temperatures for TC1 and TC2 (16 and 32 °C above ambient).

These results indicate the potential heat wastage. Between 2.9 and 5 L of water was discarded before hot water arrived; this volume of hot water would be left in the pipework afterwards. Depending on the time of year and pipe route, the heat lost from this water may contribute to space heating or may simply be wasted (Table 1, final row). The time delay ranged from 17 s (house 1) to 47 s (house 3). Measures to reduce this inconvenience as part of a move towards modern heat pump systems could raise customer satisfaction and encourage householders to switch from gas boilers.

3. Options for reducing the hot water delivery delay and heat losses

A number of alternatives could in theory achieve the desired rapid arrival of hot water and some reduction in heat loss, Fig. 2.

Fig. 2(a) shows a system with a booster pump to raise the hot water pressure. Such pumps are commonly used in houses with low water pressure to provide a pressurised shower supply; they can also be used to achieve a suitable tap flow rate through a small bore pipe. The reduction in pipe size increases the water velocity, so hot water arrives more rapidly from the thermal store. It also makes the insulation more effective, for a given external diameter, thus reducing heat losses.

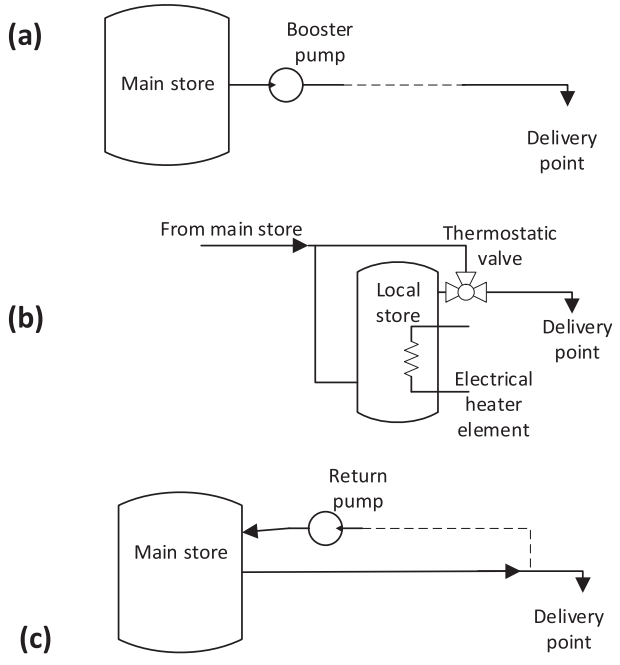

Fig. 2. Systems for reducing the wait period: (a) Small bore pipe with booster pump, (b) local heat store with heating element, (c) Circulating flow to keep pipe warm. Dashed lines indicate a small bore pipe.

Fig. 2(b) shows a local heat store that can provide instantaneous hot water.

Fig. 2(c) shows a system with a circulating pump to maintain a small flow through the hot pipework. The return pipe can be much smaller than the main pipe since it does not need to supply the tap flow; with the pump located near the main store, a single pump could be used to circulate more than one loop. The pump would ideally be controlled by a timer to warm the pipes at times of day when hot water was usually required; it could also be turned on by a sensor in response to people entering the bathroom. A similar system on a much larger scale was proposed by Bøhm [4] for hot water supply in blocks of flats. If the pressure drop were sufficiently low the circulation could be generated very simply using a thermo-syphon.

This paper is concerned with the optimal design of such a recirculation loop. The reasons for preferring this over the alternatives (small-bore pipework or local heat stores) are briefly discussed below.

3.1. Small-bore pipe with a booster pump

The booster pump concept, Fig. 2(a), provides sufficient water pressure to allow the use of a small bore pipe, thereby increasing the insulation thermal resistance (for a given sleeve diameter) and minimising the volume of water that must pass through a tap before hot water arrives from the store.

As an example. a simple pressure drop calculation indicates that delivering 0.15 L/s though a 15 m pipe length of 8 mm bore pipe would require 56 W overall pumping power to overcome a frictional pressure drop of 1.9 bar. A typical shower booster pump such as the Grundfos SSR2-2.0 has a 280 W motor and can generate a pressure rise of 1.5 bar at a flow of 0.15 L/s. Together with the water supply pressure, this would be enough to deliver the above flow rate through a pipe of 8 mm bore, so such a solution is entirely feasible using available hardware.

Water velocity in the pipe is however limited by noise and erosion considerations. Garrett [14] recommends a velocity limit for water at 50 °C of 3 m/s for accessible pipes and 1.5 m/s for pipes that cannot easily be replaced, commenting also that velocities should be limited to reduce noise.

3 m/s would supply 0.15 L/s through an 8 mm bore pipe and any higher flow rate would require larger pipe, e.g. 0.5 L/s for a bath would require at least 14.6 mm bore. The degree to which pipe size could be reduced is thus constrained by noise and erosion limits rather than pressure drop. The traditional pipe sizes of 15 and 22 mm OD (13.6 and 20.6 mm bore) with a velocity of 1.5 m/s would deliver 0.22 and 0.5 L/s respectively, indicating that there is little potential to use pipes significantly smaller than the current standard.

3.2. Local store and/or instantaneous heating at the delivery point

The second option for reducing the hot water delay would be to have an electric heater close to the delivery point, Fig. 2(b). This could either be a low-power heater to maintain a buffer tank at the required temperature or a high-power instantaneous heater without a tank.

A buffer tank would require valves so that cold water would initially enter the tank, to replace hot water leaving the tap, before switching to direct delivery once hot water arrived from the main store. An instantaneous heating system would not require valves and also avoids any heat losses from a continuously heated buffer tank. Such stores/heaters are available from manufacturers such as Insinkerator and Quooker, though they are typically used to generate hot water from a cold water feed rather than to avoid a delay in hot water delivery. Vanthournout [35] describes an electrically heated 2.4 kWh hot water buffer tank with a control algorithm for integration into a demand response system.

3.2.1. Heat losses from a local heat store

The specifications for a typical local heat store (Insinkerator 3574, 2.5 L tank, polystyrene insulation) quote a standby power consumption of 19.4 W when set to 99 °C i.e. it provides some background heating to the house at a cost of order £20p.a. at typical UK electricity prices. The Quooker equivalent uses vacuum insulation to achieve a standby power of just 10 W.

A similarly-sized store to supplement the hot water delivery for a short period until water arrives from the main store could operate at 60 °C i.e. halving the temperature difference to ambient. Heat loss rates in the range 5–10 W should therefore be achievable.

A store to deliver hot water during the transit time period would need to hold about 7 L of water (volume of 22 mm OD copper pipe × 20 m long = 6.7 L is a conceivable "worst case"). As it delivered its hot water it would fill with the ambient-temperature water from the cold pipe until hot water arrived from the main store and the thermostatic valve switched to accepting piped rather than stored hot water. The local store would then need to heat to a suitable delivery temperature of at least 40 °C whilst the water in the pipe was hot enough for the store to be unnecessary.

A simple conduction calculation for the heat losses from an insulated, water-filled pipe with free convection to surrounding air can be integrated over the time since flow ceased to give a mean heat loss rate, Fig. 3. The design case here is Knauf HPS insulation (chosen for its durability; k = 0.035 W/mK) with an external diameter of 75 mm and an initial temperature difference of 40 °C (e.g. water 60 °C, ambient 20 °C). The convection correlation models the insulation surface as a horizontal cylinder at uniform temperature.

The cooling curves in Fig. 3 show that the mean heat loss rate to 40 °C ("+" marker on curves) is 52 W for 15 mm pipe and 66 W for 22 mm pipe over a typical 15 m length. These values indicate the minimum acceptable power to reheat cold water in the local store, not including the store's own heat loss rate.

3.2.2. Power required for an instantaneous heater.

Electric showers for a cold water supply are typically rated between 8.5 and 10.5 kW and require a 10 mm^2 cable connected to a dedicated circuit breaker in the consumer unit. A similar heating element could supply instant hot water to taps: at a flow rate of 0.1 L/s, 8.5 kW is sufficient to raise the temperature by 20 °C. The requirement for a higher flow rate when filling a basin or bath is

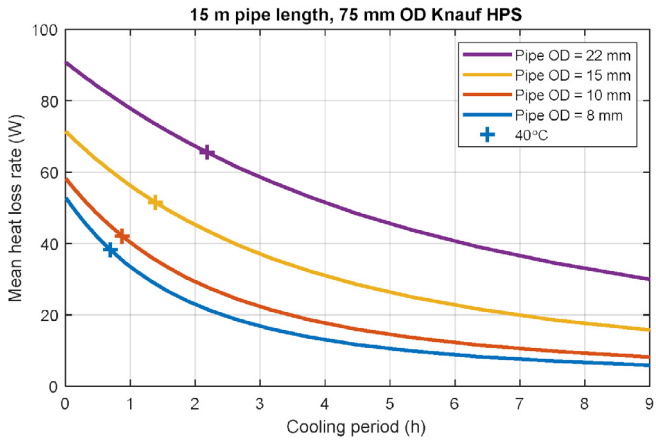

Fig. 3. Time-mean heat loss rates for insulated pipes as a function of cooling period and pipe diameter.

less temperature-sensitive since hot water from the main store will typically arrive in time to achieve the desired final temperature.

The desired user experience could therefore be achieved using either a low-power local heat store or a high-power instantaneous heater. Both these options require direct electrical heating to balance the heat losses and are a less efficient option than generating the required heat using a heat pump. They also require bathroom or kitchen space to house the buffer tank.

3.3. Benefits of a recirculation system

A recirculating system would overcome the above difficulties, Fig. 2(c). No additional equipment is required at the delivery point and any heat loss from pipework to indoor space would be replenished by the heat pump rather than electrical heating.

The simulation code for analysis of recirculating systems was developed from a non-recirculating, single-pass model. Section 4 below describes the single-pass transient flow model, compares it with previous work in this field and validates it against an analytical solution. Section 5 introduces the double-pass concept with a steady-state heat transfer solution and describes an optimal insulation distribution based on the steady-state analysis. Section 6 describes the extension of the transient model to a two-pass system and calculates the necessary flow rate to achieve warm-up after 1–2 h. Section 7 compares the heat losses for recirculating and conventional systems and discusses the possibility of a pumpless thermo-syphon system.

4. Transient flow calculations for a single pipe.

Fig. 1 has demonstrated some typical delay times due to the hot/cold water interface convecting along a pipe. The authors were curious about these curves: were the observed profiles largely due to heat transfer effects, or were they the result of turbulent mixing across the interface due to the radial velocity profile?

4.1. Prior work: Advection modelling assuming equal water and pipe temperatures

The heat capacity of the pipe wall will initially cool the hot water leaving the thermal store. Thermo-hydraulic pipe models that account for pipe heat capacity and convection losses have been developed by Gu [16], Gabrielaitiene [13] and van der Heijde [33]. Gu assumed constant temperature over a cross-section (equal pipe and water temperatures i.e. an infinite water-pipe heat transfer coefficient); the advection equation is:

$$\dot{c}_w \frac{\partial T}{\partial x} + c_{wp} \frac{\partial T}{\partial t} + HT = HT_\infty \qquad [10]$$

Gu solved this equation for a step change in inlet temperature to obtain:

$$T(x,t) = T_\infty + \left[(T_{inlet} - T_\infty)e^{-\frac{Hx}{\dot{c}_w}} - (T_0 - T_\infty)e^{-\frac{Ht}{c_{wp}}}\right] u\left(t - \frac{c_{wp}}{\dot{c}_w}x\right) + (T_0 - T_\infty)e^{-\frac{Ht}{c_{wp}}}$$

where $T_0 = T(x,0)$ is the initial pipe temperature, T_∞ is the air temperature and $T_{inlet} = T(0,t)$. [11]

This predicts the temperature variation with time for both the pre- and post-interface regions. The effect of the pipe wall heat capacity is to make the speed of the hot/cold interface (represented by the step function in equation [11]) less than the water velocity.

This behaviour might appear to be counter-intuitive as experience suggests that the water at the delivery point does not suddenly jump from cold to hot. Reasons for this observed behaviour will be discussed below.

The reduced velocity and sudden step at the hot/cold interface in Gu's analytical solution can be explained by considering a control volume around the interface region and representing this volume as a heat exchanger. Since the heat transfer coefficient in Gu's solution was assumed to be infinite, the virtual heat exchanger effectiveness would be $\varepsilon = 1$.

The speed of the interface is then such that the heat capacities of the water (left to right in Fig. 4) and the metal (treated as a fluid with relative motion from right to left) are equal in the moving frame of reference, in accordance with the step function in equation [11]:

$$(\rho Ac)_w (v_w - v_i) = (\rho Ac)_m v_i$$

$$v_i = \frac{v_w}{\left[1 + \frac{(\rho Ac)_m}{(\rho Ac)_w}\right]} \qquad [2]$$

This solution is obtained if the water and metal are equal in temperature over the cross-section. It will be shown below that it also closely approximates the interface velocity in the finite heat transfer coefficient case.

Gu [16] transformed the PDE [10] into a finite difference equation, using an implicit forwards-difference iteration scheme:

$$T_{w,i,c} = \frac{\frac{\dot{c}_w T_{i-1,c}}{\Delta x} + \frac{c_{wp} T_{i,p}}{\Delta t} + HT_\infty}{\left(\frac{\dot{c}_w}{\Delta x} + \frac{c_{wp}}{\Delta t} + H\right)} \qquad [3]$$

Iteration scheme [3] is incapable of accurately representing a temperature step at the hot/cold interface and trials of this scheme with different step lengths showed the length of the hot/cold interface reducing as the step length was diminished. Gu commented that the numerical solution was closer to experimental results than the analytical solution: it may be coincidental that the numerical smearing mimicked the experimental effects of finite heat transfer.

4.2. Prior work: Modelling heat transfer between water and pipe

In practice the heat transfer coefficient between water and pipe wall is proportional to the convective flow Nusselt number and cannot safely be assumed to be infinite. For time periods short enough that the pipe can be considered isothermal, the water temperature will obey the equation [11] with the pipe mass set to zero; effectively the pipe becomes the environment, T_∞ is then the pipe wall temperature and H is the water-pipe heat transfer coefficient, giving a sharp step in water temperature which moves at the flow velocity v_w.

Typical time constants for the pipe wall are however in the range 0.3–1 s; beyond this time the wall temperature variation will have a significant effect on water temperatures i.e. the equation needs to model the water and pipe temperatures separately. Even

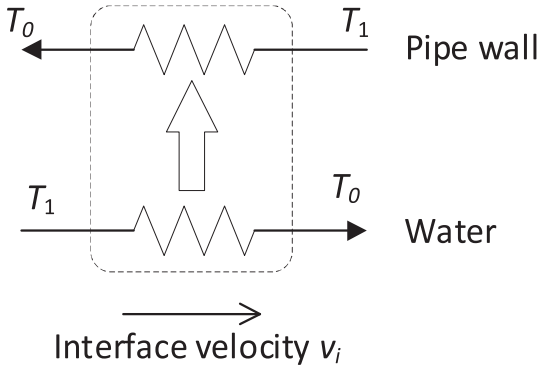

Fig. 4. The velocity of the hot/cold interface in the analytical solution with infinite water to pipe heat transfer coefficient may be explained in terms of a virtual heat exchanger.

then, great accuracy is not to be expected since the water temperature will also be affected by the velocity profile across the pipe and by the initial temperature distribution. For systems controlled by a tap at the far end, axial conduction and free convection in the open pipe close to the thermal store means there will not be a sharp hot/cold interface entering the pipe as the flow starts (e.g. the House 2 data in Fig. 1).

A finite wall heat transfer coefficient may be modelled by expanding equation [10] as a pair of linked differential equations for mean water temperature $T_w(x,t)$ and pipe temperature $T_p(x,t)$:

$$\begin{aligned} \dot{c}_w \tfrac{\partial T_w}{\partial x} + c_w \tfrac{\partial T_w}{\partial t} + hT_w &= hT_p \\ c_p \tfrac{\partial T_p}{\partial t} + (h+H)T_p &= hT_w + HT_\infty \end{aligned} \quad [4]$$

This is a plug flow model i.e. with uniform water temperature over the pipe cross-section. h is the water to pipe heat transfer coefficient and H is the pipe to environment heat transfer coefficient (including any insulation). The analytical solution to [4] for a uniform pipe subject to a step in inlet temperature is given by Vedat [36] in terms of the integral of a modified Bessel function:

$$\begin{aligned} T_w &= (T_{inlet} - T_\infty)e^{-b_1 t_0}\left(e^{-b_4 t^*} I_0\left(2\sqrt{b_1 b_2 t_0 t^*}\right) + b_4 I^*\right) + T_\infty \\ T_p &= (T_{inlet} - T_\infty) b_2 e^{-b_1 t_0} I^* + T_\infty \end{aligned} \quad [5]$$

where $t_0 = \frac{x}{v_w}$, $t^* = t - t_0$, $b_1 = \frac{h}{c_w}$, $b_2 = \frac{h}{c_p}$, $b_3 = \frac{H}{c_p}$, $b_4 = b_2 + b_3$ and $I^* = \int_0^{t^*} e^{-b_4 s} I_0\left(2\sqrt{b_1 b_2 t_0 s}\right)\, ds$.

Solution [5] gives a time-varying water temperature as opposed to the sudden step in equation [11]. As time tends to infinity the temperature distribution approaches the steady state component from equation [11]:

$$T_w = (T_{inlet} - T_\infty)e^{-\frac{Ux}{c_w}} + T_\infty \quad [6]$$

and $T_p = \frac{U}{H}(T_{inlet} - T_\infty)e^{-\frac{Ux}{c_w}} + T_\infty$ where the overall heat transfer coefficient $U = \left(h^{-1} + H^{-1}\right)^{-1}$ W/mK.

4.3. Method of Lines transient model for a single pipe

Vedat's solution [5] for a uniform pipe allows the accurate determination of hot water arrival time in the classical situation i.e. the sudden start of hot flow into a cold pipe.

The proposed recirculating system using a pair of pipes (possibly sharing a common insulation sleeve) required an inter-pipe heat leakage term adding to equation [4]. The equations then become too complex for analytical solution but can easily be solved using the linked ODE solvers in Matlab. The code models the 1-D temperature changes in a constant flow rate pipe flow, assuming time-steady heat transfer coefficients: it solves the temperature equations rather than the Navier-Stokes fluid flow equations.

The development of a solution scheme started by validating code for the single pipe case.

Initial attempts to extend Gu's iterative scheme [3] to include both pipe and water temperature suffered from numerical smearing of the temperature jump due to discretization of $\frac{\partial T}{\partial x}$ across the step and were moreover very computationally expensive (8 Gb memory required to simulate 4 m of pipe with a 0.2 mm step length, increasing as the square of the pipe length).

To overcome the smearing and memory limitations, equation [4] was subsequently solved using a "Method of Lines" approach [19] which converts the PDE into a system of linked ordinary differential equations. Attempts to simulate [4] using the Method of Lines on a static grid suffered from instability near the temperature step. To avoid this, the system of equations was re-defined using a static grid x for the metal nodes and a moving grid y (with nodes translating past x at the water velocity) for the water. This is a Lagrangian model [28]. Since the grid moves with the flow, the advection $\frac{\partial T}{\partial x}$ term disappears.

The code does not model axial conduction within the water or the pipe wall. There is therefore no need for the 1D grid to be fine enough to define temperature gradients in the axial direction: it only needs to be sufficient for accurate linear interpolation of the temperatures between the static and moving nodes. The justification for omitting any axial conduction is that the pipe will typically be much longer than the penetration depth of a thermal conduction wave, in water or copper, over the simulated flow period. The penetration depth will be of order $\sqrt{\pi \alpha t}$ (0.15 m after 1 min for copper, 5 mm for water). This is much less than a typical pipe length of 15 m and, since conduction is a linear process, small conduction-induced changes to the local axial temperature distribution around the hot/cold interface will not significantly affect the total heat transfer from water to pipe.

The ODEs for a water node i and a pipe node j are:

$$\begin{aligned} c_w \tfrac{dT_{w,i}}{dt} + hT_{w,i} &= hT'_{p,i} \\ c_p \tfrac{dT_{p,j}}{dt} + (h+H)T_{p,j} &= hT'_{w,j} + HT_\infty \end{aligned} \quad [7]$$

where at each time step $T'_{p,i}$ is the pipe temperature interpolated onto the water grid at the water node i position and $T'_{w,j}$ is the water temperature interpolated at pipe node j. To ensure realistic values of $T'_{p,j}$ and $T'_{w,j}$ for all grid points throughout the iteration at times up to $2t_0$ the pipe grid extends to $x = 2L$ and the water grid covers the range from $y = \{-2L, 2L\}$.

The system of equations was solved numerically using Matlab's ODE23S Euler-solver for systems of linked equations [30,31]. The required Relative Tolerance was set to 10^{-5} so each output value should be an accurate solution of the equations (as defined in terms of numerical derivatives based on the discrete values) to within ±0.001%. ODE23S automatically determines the necessary time step to achieve this accuracy whilst it iterates. The coding requirement is therefore limited to defining the system of equations rather than implementing any kind of iteration scheme.

The initial conditions were $T_p(t=0) = 20°C$ and $T_w(x=0, t>0) = 60°C$.

Typical solutions are shown in Fig. 5. If the water velocity changes due to non-uniform pipe diameter the separation of the water nodes will vary in proportion to the speed ratio; the heat capacity c_w(J/mK) also changes.

The lines of pipe temperature in Fig. 5 show the time history produced by the Method of Lines solution at each × node; the water temperature surface includes lines of constant time and constant y. The water temperature exhibits an "initial step" region in which the temperature jumps suddenly when the hot water arrives. This temperature jump reduces in amplitude with distance along the pipe; as it does so, the subsequent water temperature rise with time due to warming of the pipe becomes more significant. This interpretation is also evident from the two T_w terms in equation [5].

Fig. 6 shows the propagation velocity along *iso*-temperature lines. This velocity drops below the flow velocity at the end of the initial step region and is thereafter close to the interface velocity from [2].

Van der Heijde [33] used a thermal capacitance model with the heat capacity of the pipe added at pipe exit. Fig. 7(a) compares this approach to the Method of Lines solution from Fig. 6. Two capacitance models have been compared:

- treating the pipe heat capacity as an equivalent mass of water and applying a 'mix and discard' model (infinite heat transfer coefficient) at the exit, as van der Heijde. This is the 'Lumped mix' in Fig. 7(a).

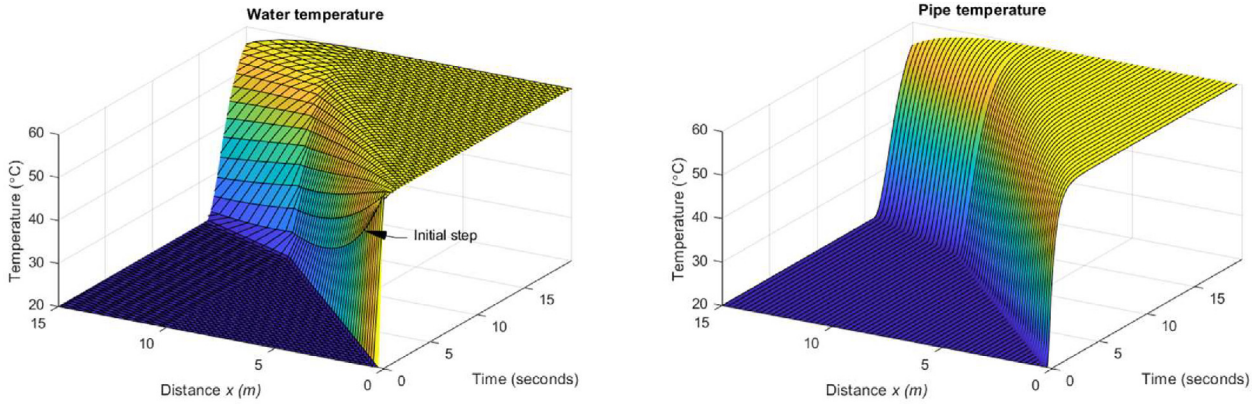

Fig. 5. Typical "Method of Lines" solution to equation (8) for 0.25 kg/s through 10 m of 22 mm OD copper pipe followed by 5 m of 15 mm pipe: water 60 °C, environment 20 °C, 15 mm insulation thickness with $k = 0.035$ W/mk.

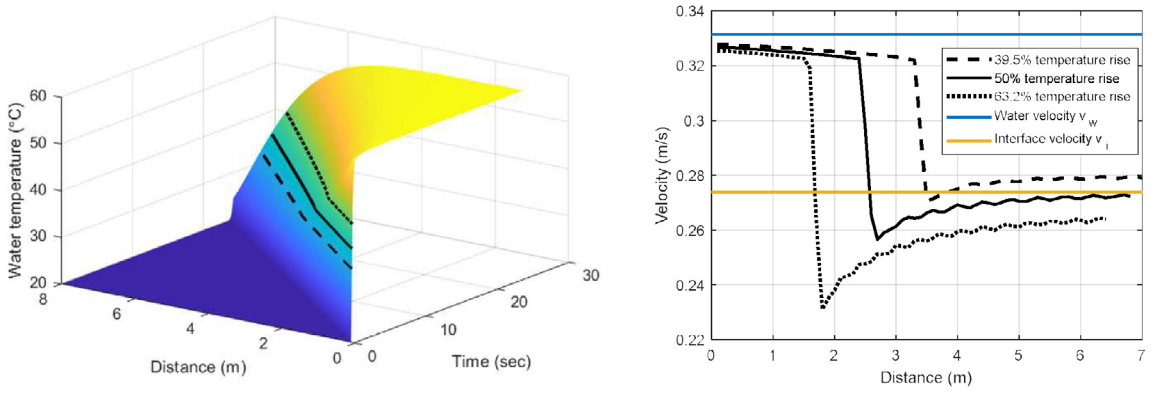

Fig. 6. Method of Lines solution comparing the interface velocity (lines across the surface) with the flow and interface velocities from equation [2] for $T_w = T_0 + f(T_{inlet} - T_0)$, $f = \{1 - e^{-0.5},\ 0.5,\ 1 - e^{-1}\}$. (Conditions as Fig. 5).

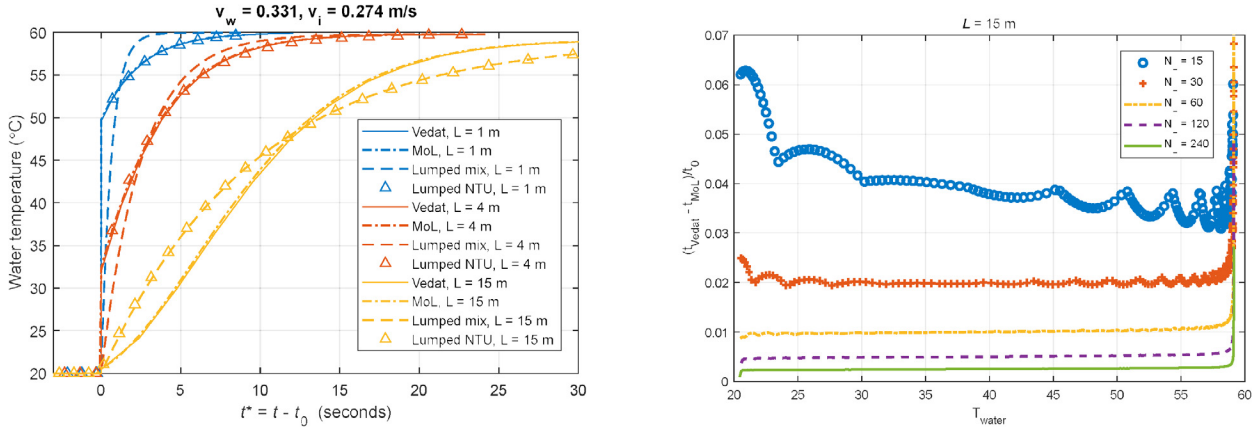

Fig. 7. (a) Exit temperature–time profiles after a step change in inlet temperature, comparing the analytical solution (Vedat) with Method of Lines and lumped capacitance models for three pipe lengths. (b) Time delay error relative to the analytical solution (N_L = number of grid points, to × = L).

- a heat exchanger "NTU" model of pipe and water temperature, giving effectiveness $\varepsilon = 1 - e^{-NTU}$ for heat transfer between water and a uniform temperature pipe. This is the 'Lumped NTU' in Fig. 7(a).

The results in Fig. 7(a) are the time history of the water temperature at 3 locations along the pipe (or at exit from 3 pipes of different lengths: 1, 4 and 15 m). To facilitate comparison the curves have been time-shifted by the water arrival times $t^* = t - t_0$ where $t_0 = 3.02$, 12.08 and 45.3 s respectively.

In terms of the wait time before hot water arrives, all these models produce useful results; high accuracy is not necessary. The "Lumped mix" model however fails to reproduce the analytical temperature rise curves.

An alternative lumped thermal capacity model was used by Wojtkowiak [38]. He noted though that his analytical solution for heat transfer between water and a uniform temperature pipe failed to match experimental pipe flow measurements.

The Method of Lines solution in Fig. 7(a) is very close to the analytical curve; the water temperature is very slightly over-predicted (a grid-dependent effect). The "Lumped NTU" model is close to the exact solution for short pipes but deviates towards the Lumped Mix model as pipe length increases.

Fig. 7(b) investigates grid-dependence for the method of lines algorithm. The hot water arrival time was slightly less than for the analytical solution. The graph shows this time error, as a fraction of the water propagation time t_0, plotted against water temperature i.e. the y-axis in Fig. 7(b) corresponds to the x-axis in 7 (a). $N_L = 60$ grid points over the pipe length were sufficient to give a time error of order 1% which is more than adequate for the intended purpose of ranking insulation options and identifying the necessary flow rate and optimum geometry. The computational grid for the pipe actually extends beyond the nominal pipe length for convenience when interpolating from the water grid and similarly the water grid starts before the pipe start, to allow it to slide past the pipe grid.

The hot/cold interface will also gradually spread in length due to diffusion and turbulent mixing: these are not modelled in the simulation. Chertkov [7] estimates this interface width as $\Delta L = \sqrt{dL} = L\sqrt{\frac{d}{L}}$. For L/d = 1000 this would only add about 3% to the effective pipe length.

The Method of Lines predictions compared with experimental data in Fig. 1 model the variations in diameter (a combination of 15 and 22 mm OD), wall thickness and material along the length of each pipe. These parameters are estimated because it was not possible to gain access to the full length of the pipes without removing plasterboard and floorboards.

The House 2 kitchen spur includes a section of PEX pipe, the remainder being copper. The measured hot-water arrival period is slightly broader than predicted. This is thought to result from mixing due to the velocity profile across the pipe: equation [7] assumes plug flow.

The water arrival time for the House 2 bathroom in Fig. 1 is less than predicted. This could simply indicate that the flow rate varied slightly during the test.

5. Viability and optimisation of a recirculating system

Circulation systems keep the pipes hot via a continual flow of hot water. This could well be controlled by an "intelligent" system, either on a timer to warm pipes at particular times of day or via sensors that detected entry to the bathroom and kitchen.

The required flow rate depends on the allowable temperature drop along the pipe, the heat loss rate and the heat transfer between outward and return flows. Heat transfer between flows is not desirable but will always be present to some extent particularly if, for convenience, the small return pipe is placed inside a common insulation jacket with the flow pipe. Such systems have been investigated on a district heating scale with identical pipe diameters by van der Heijde [34]; the present case includes dissimilar pipes and thermal resistance between pipes and water.

5.1. Steady-state algebraic solution

The case of a double-pass system with good thermal contact between the two streams has been studied by Moss [25] in a solar collector context with uniform heat flux. The pipe flow equivalent with three independent thermal resistances is shown in Fig. 8.

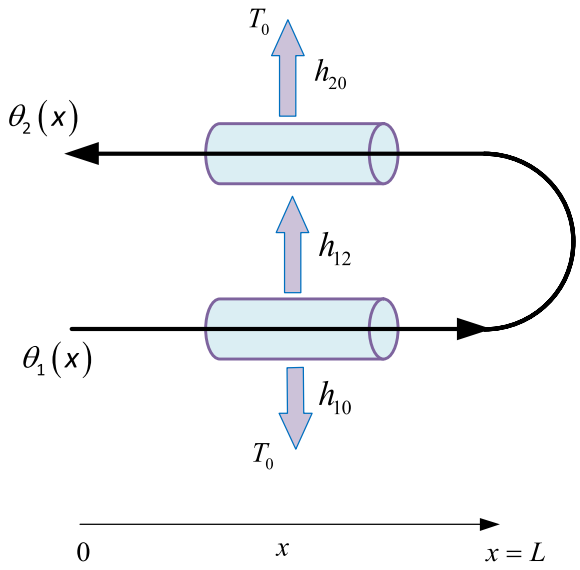

Fig. 8. Geometry of a circulating system with equal flow rates $\dot{m}$ in each direction (no discharge through taps). The three thermal conductances correspond to the thermal resistance components used by van der Heijde [34].

Denoting the outward and return flows as 1, 2 respectively, the water temperatures are θ_1, θ_2 and overall heat transfer coefficients per unit pipe length are h_{10}, h_{20} to the external air and h_{12} between the tubes. Only the case with no delivery discharge has been modelled because the analysis is intended to show the necessary recirculation rate to maintain a set end-point temperature.

To solve the time-steady case the time derivative in the general advection equation $\dot{c}_w \frac{\partial T}{\partial x} + c_{wp} \frac{\partial T}{\partial t} + HT = HT_\infty$ is set to zero. There is no need for a differential equation for the pipe temperature since in the steady state this is linearly related to the water temperature via the thermal resistances. There is then a pair of linked equations for the water in each pipe:

$$\dot{c}_w \frac{d\theta_1}{dx} + (h_{10} + h_{12})\theta_1 = h_{10}T_0 + h_{12}\theta_2$$

$$-\dot{c}_w \frac{d\theta_2}{dx} + (h_{20} + h_{12})\theta_2 = h_{20}T_0 + h_{12}\theta_1$$

These equations have previously been solved algebraically [34]. The present solution is perhaps more convenient in that it achieves the same result using eigenvectors.

In matrix form,

$$\begin{bmatrix} \dot{\theta}_1 \\ \dot{\theta}_2 \end{bmatrix} = \frac{1}{\dot{c}_w} \begin{bmatrix} -(h_{10} + h_{12}) & h_{12} \\ -h_{12} & (h_{20} + h_{12}) \end{bmatrix} \begin{bmatrix} \theta_1 \\ \theta_2 \end{bmatrix} + \frac{1}{\dot{c}_w} \begin{bmatrix} h_{10} \\ -h_{20} \end{bmatrix} T_0$$

The solution can be written as the sum of a homogeneous and non-homogeneous term:

$$\theta_i = \theta_{i,h} + \theta_{i,nh}, \quad i = 1, 2 \qquad [8]$$

The homogeneous part is $\begin{bmatrix} \dot{\theta}_{1h} \\ \dot{\theta}_{2h} \end{bmatrix} = \frac{1}{\dot{c}_w} \begin{bmatrix} -(h_{10} + h_{12}) & h_{12} \\ -h_{12} & (h_{20} + h_{12}) \end{bmatrix} \begin{bmatrix} \theta_{1h} \\ \theta_{2h} \end{bmatrix}$ which can be written in matrix form as $\dot{\theta}_h = \boldsymbol{A}\theta_h$.

The non-homogeneous part is the solution of a simultaneous equation:

$\begin{bmatrix} -(h_{10} + h_{12}) & h_{12} \\ -h_{12} & (h_{20} + h_{12}) \end{bmatrix} \begin{bmatrix} \theta_{1nh} \\ \theta_{2nh} \end{bmatrix} = -T_0 \begin{bmatrix} h_{10} \\ -h_{20} \end{bmatrix}$ with solutions

$$\begin{bmatrix} \theta_{1nh} \\ \theta_{2nh} \end{bmatrix} = -T_0 \begin{bmatrix} -(h_{10} + h_{12}) & h_{12} \\ -h_{12} & (h_{20} + h_{12}) \end{bmatrix} \{ \begin{bmatrix} h_{10} \\ -h_{20} \end{bmatrix}$$

The homogeneous solution will be of the form $\theta_h = ae^{\lambda_a x}\boldsymbol{v}_a + be^{\lambda_b x}\boldsymbol{v}_b$ where λ_a, λ_b are the eigenvalues of A and $\boldsymbol{v}_a$, $\boldsymbol{v}_b$ are corresponding eigenvectors, $\boldsymbol{v}_a = \begin{bmatrix} v_{a1} \\ v_{a2} \end{bmatrix}$. The constants a, b are set by the boundary conditions:

- $ae^{\lambda_a 0}\boldsymbol{v}_{a1} + be^{\lambda_b 0}\boldsymbol{v}_{b1} = \theta_1(0)$ at $x = 0$
- $\theta_1(L) = \theta_2(L)$ hence $ae^{\lambda_a L}(\boldsymbol{v}_{a1} - \boldsymbol{v}_{a2}) + be^{\lambda_2 L}(\boldsymbol{v}_{b1} - \boldsymbol{v}_{b2}) = 0$

a, b are then the solution to a matrix equation:

$$\begin{bmatrix} \boldsymbol{v}_{a1} & \boldsymbol{v}_{b1} \\ e^{\lambda_1 L}(\boldsymbol{v}_{a1} - \boldsymbol{v}_{a2}) & e^{\lambda_2 L}(\boldsymbol{v}_{b1} - \boldsymbol{v}_{b2}) \end{bmatrix} \begin{bmatrix} a \\ b \end{bmatrix} = \begin{bmatrix} \theta_{1h}(0) \\ 0 \end{bmatrix} = \begin{bmatrix} \theta_1(0) - \theta_{1nh}(0) \\ 0 \end{bmatrix} \quad [9]$$

Equations [9,10] enable the steady-state temperature distribution to be evaluated in Matlab using just 10 lines of code.

5.2. Relationship between 'common sleeve' insulation geometry and required flow rates

Fig. 9 shows the effect of geometrical parameters on the above heat transfer coefficients h_{10}, h_{20} and h_{12} which have been obtained via PDE conduction solutions for a pair of flow and return pipes sharing a common insulation sleeve (Appendix A). f, g, m and n are non-dimensional parameters defining the pipe size ratio, combined pipe size as a fraction of the insulation diameter, central gap and minimum distance from the surface to the main pipe.

A sleeve outer diameter of 75 mm was chosen as the largest size that might be practical in a domestic context, with a thermal conductivity of 0.035 W/mK for ease of comparison with the single pipe analysis in Section 3.2.

Fig. 10 shows the steady-state water temperature distribution along the flow (solid line) and return (dashed line) pipes for a nominal geometry at 5 different flow rates. The geometry corresponds to the $m = 0.3$, $n = 0.5$ point on the Fig. 9 surfaces. Raising the flow rate reduces the temperature difference between the flow entering and leaving the system.

Fig. 10 shows that a flow rate of 0.6 cm^3/sec would be enough to maintain a temperature of at least 40 °C at the end of a 15 m long delivery pipe, based on a nominal geometry. Fully developed laminar flow has been assumed. (A flow of 1 cm^3/s at 40 °C would give

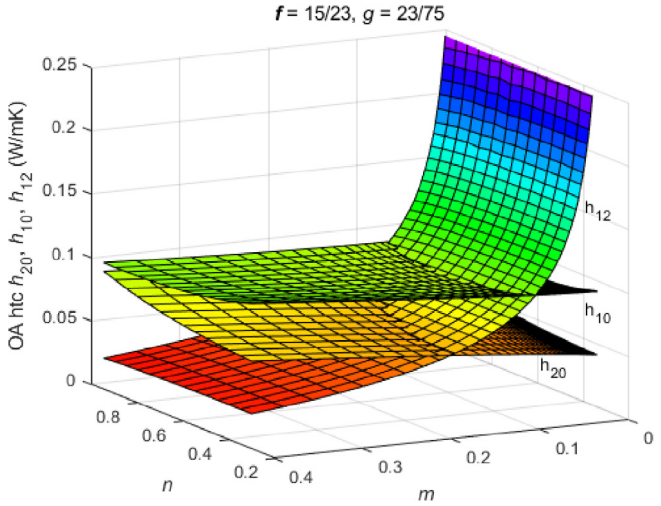

Fig. 9. Overall heat transfer coefficients per metre length, water–air and water-water, for various positions of 15 and 8 mm diameter pipes within a horizontal 75 mm diameter sleeve, $k = 0.035$ W/mk. Laminar flow with $Nu = 4.36$ internally; $h_{ext} = 3.9$ W/m^2K(typical for air-side $\Delta T = 5$°C).

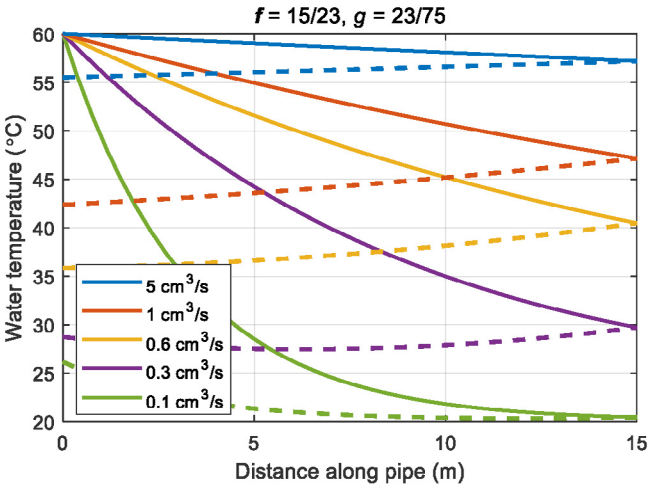

Fig. 10. Effect of flow rate on steady-state water temperatures for a pair of 15 m long, 15 and 8 mm OD pipes, based on heat transfer coefficients from Fig. 9 at $m = 0.3$, $n = 0.5$ (27.4 mm centres, equal minimum insulation thickness for each pipe to air). $T_0 = 20$°C and $T_{IN} = 60$°C.

Reynolds numbers of 143 and 295 in pipes of 15 and 8 mm OD and the thermal entry lengths, calculated as $\frac{L}{d} = 0.05RePr$, would be 0.43 m in each case. Recirculation rates of up to 6.8 cm^3/s would therefore be expected to give laminar flow (Re < 2000): these flows are very small compared to the much higher rates when water is taken from the tap).

Fig. 11 shows how variations in geometry affect the heat loss and the flow required to sustain this 40 °C end-point temperature.

5.3. Optimisation of common sleeve insulation geometry

For each pipe spacing (parameter m in Figs. 9 and 11) there will be an optimum pipe offset value n to achieve minimum heat loss, given that the flow rate has been set to achieve 40 °C at the pipe end. This is illustrated in Fig. 12.

For a small increase in heat loss rate from 50 to 52 W, the mass flow can be reduced from 0.79 to 0.59 g/s if m is increased from 0.01 to 0.1. Values of m below 0.01 were not used, to avoid having to estimate a contact resistance if the two pipes were in contact; such solutions would also deserve more detailed modelling to include conduction around each pipe. At m = 0.1 the optimum pipe offset is n = 0.576.

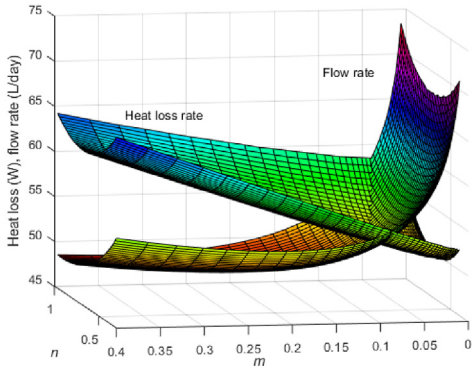

Fig. 11. The minimum heat loss for given temperature (40 °C) at $x = L$ occurs when the two pipes are as close together as possible ($m \approx 0$). For gridding purposes, the smallest m value was taken as 0.01. Heat transfer between the pipes increases the required flow rate as $m \to 0$.

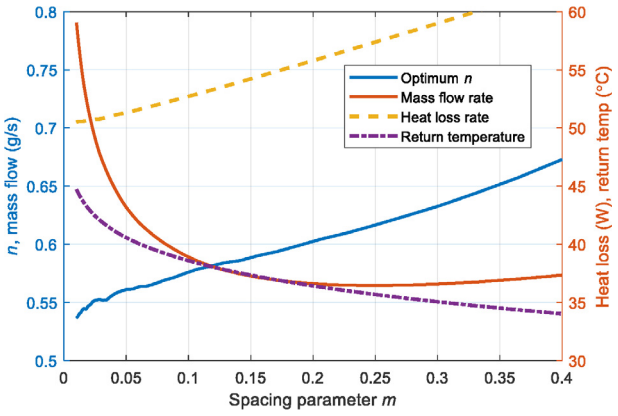

Fig. 12. Optimal pipe offset in terms of pipe spacing; other parameters as Figs. 9 and 11.

If laminar flow is required, e.g. to avoid noise, there will be a limit on the allowable flow rate or minimum pipe size. $Re = \frac{4\dot{m}}{\pi d\mu}$ hence a Reynolds number limit of 2000 implies $\frac{\dot{m}}{d} = 500\pi\mu$. The viscosity of water varies slightly with temperature: it is convenient to remember that $\frac{\dot{m}}{d} = 1$ kg/ms gives $Re = 2000$ at a temperature of 41.6 °C e.g. 0.006 kg/s through a 6 mm bore pipe.

5.4. Comparison between common sleeve and separate pipe geometry

The previous sections have assumed that a common sleeve would provide better insulation than separate pipes each with their own sleeve. The validity of this assumption is demonstrated by the simulation in Fig. 13 for two separate pipes with a combined outer diameter (over both insulation sleeves) of 75 mm. The analysis was performed for two conditions, achieving temperatures of 40 °C and 50 °C at the delivery point.

The insulation fraction n for separate tubes is analogous to the common sleeve definition:

$n = \frac{A}{A+B}$ where A, B are the insulation thicknesses on the flow and return pipes.

For simplicity, the two pipes in Fig. 13 have been assumed to be completely separate, with no physical contact, so that $h_{12} = 0$ and the overall heat transfer coefficient for each pipe is unaffected by the presence of the other pipe.

Comparing the Fig. 13 result for 40 °C delivery with Fig. 12 shows that the minimum heat loss of 89 W for separate pipes is considerably higher than the 50 W for pipes sharing a common sleeve. The required mass flow rate (in the range 0.63–0.82 g/s to maintain 40 °C at the tap) is also slightly higher than would be necessary with a common sleeve.

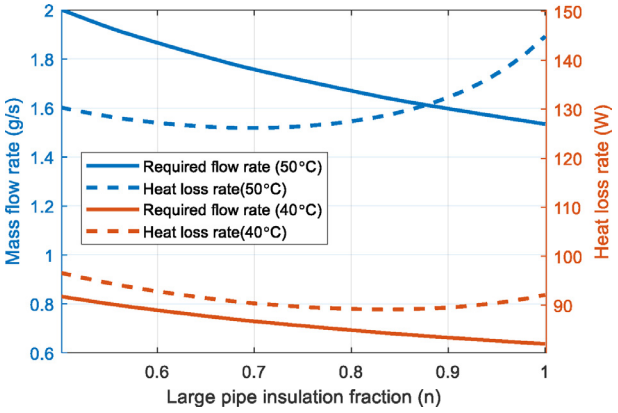

Fig. 13. Solution for two separate pipes with combined width over both insulation sleeves of 75 mm.

The pumping power required by a recirculation system would be minimal. Assuming typical copper pipe wall thicknesses of 0.6 & 0.7 mm for the 8 and 15 mm OD pipes, the 0.59 g/s from Fig. 12 would incur a frictional head loss of 11 mm and the pumping power would be approximately 60 μW. In the absence of other buoyancy effects (i.e. if the pipework were horizontal) this flow rate could be generated using a thermo-syphon with the return port 1.12 m lower on the cylinder than the outlet port. This based upon a return temperature of 36 °C, Fig. 10, and assumes a uniform 60 °C inside the hot water store.

Comparison of the 40 and 50 °C heat loss curves in Fig. 13 shows that insulating the return pipe becomes more important at the higher flow rate in the 50 °C case (the optimum n value falls from 0.84 to 0.7). This is also true for common-sleeve insulation: the optimum n falls towards 0.5 as the mass flow rate increases.

Using a greater thickness of insulation, or a lower conductivity insulation material, would clearly reduce the heat losses. The heat loss rate shown in Fig. 12 does however appear acceptable, given that an efficient heating system would be used: for a significant part of the year the heat loss would moreover contribute to the overall space heating and reduce the demand on the central heating.

6. Method of Lines transient model for a recirculating system

The Method of Lines algorithm in Section 4.3 can simulate a pipe that changes in diameter. This could be the pipe carrying hot water to the delivery point and then reducing in size before returning to the heat store. To include heat transfer between the two pipes an extra term was added to Eq. [7]:

$$c_{p,j}\frac{dT_{p,j}}{dt} + (h + H_{j,0} + H_{j,k})T_{p,j} = hT'_{w,j} + H_{j,0}T_0 + H_{j,k}T_{p,k}$$

where pipe node k is in the same cross-section as j but on the other pipe and $H_{j,k}$ is the heat transfer coefficient for pipe to pipe conduction through the insulation. The heat capacity $c_{p,j}$ is the local pipe heat capacity (for pipe j or k) plus a fraction of the bulk heat capacity of the insulation. Having defined the insulation mean temperature as $\bar{T} = a_0T_0 + a_1T_1 + a_2T_2$ (Appendix A) where T_0 is the ambient temperature and T_1, T_2 are the pipe wall temperatures, the effective increase in pipe 1 heat capacity due to the insulation will be $a_1(\rho cA)_{sleeve}$. For the insulation geometry used in Figs. 9, 11 and 12 above with m = 0.1 and n = 0.576 the coefficients are $a_1 = 0.278$, $a_2 = 0.149$. The analysis assumes that changes in temperature are gradual enough for the temperature distribution in the insulation, for any given pipe temperatures, to approximate to the steady state for those temperatures.

The unsteady water temperature, Fig. 14(a), shows both the warm front propagation as in previous figures and slight heating of the return water due to heat transfer between the outward and return fluid. The flow rate of 0.6 g/s for a 15 m pipe length would be sufficient to maintain the delivery point temperature at 40 °C (ambient 20 °C, supply at 60 °C) after tap use but the recirculating flow would either need to run continuously or commence well in advance of any demand.

The recirculation system might for instance be disabled overnight and then need to restart from cold. Fig. 14(b) shows the evolution of delivery temperature at x = 15 m as both "warm-up" curves after a cold start and "cool down" curves after a hot water delivery has raised the pipework to a uniform temperature. Comparison of the warm-up curves in Fig. 14(b) with the analytical

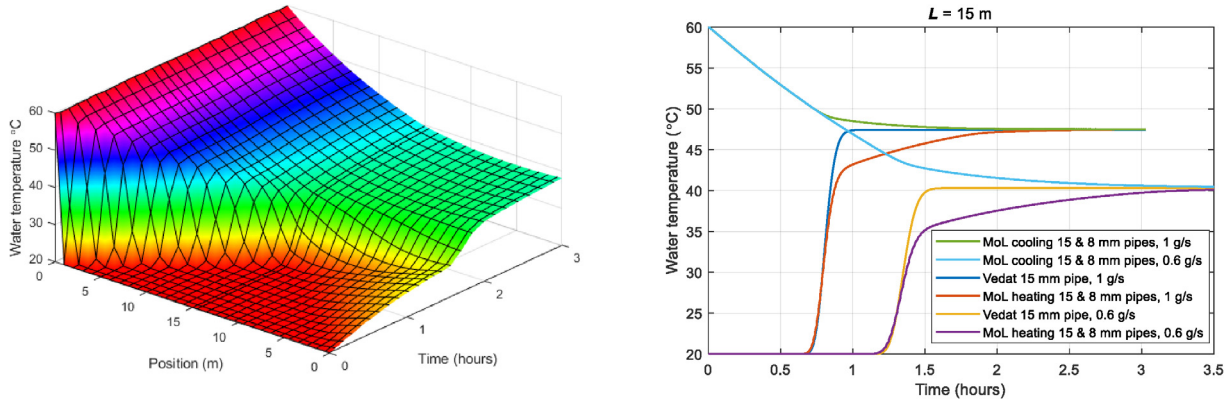

Fig. 14. (a) Water temperatures along both pipes in a recirculating system ($\dot{m} = 0.6$ g/s, flow from left to right, initially cold), (b) Method of Lines solution for delivery temperature (both "hot" and "cold" initial conditions); the latter is compared with the analytical solution for a single pipe.

solution [6,36] for a single pipe shows two phases to the warm-up process: the initial arrival of the hot water at the delivery point followed by a more gradual temperature rise as heat transfer between the flow and return pipes reduces due to the return pipe filling with hot water.

The single-pipe simulations included for comparison in Fig. 14 (b) were based on an overall heat transfer coefficient U chosen to give the same steady-state delivery temperature in [6] as given by equations [9,10] for the recirculating system in Fig. 14(a). Keeping the water to pipe heat transfer coefficient h unchanged, the appropriate U value was achieved using $H = H_{01} + fH_{12}$ where $f \approx \{0.32, 0.22\}$ at 0.6 and 1 g/s respectively.

The transient analytical solution for a single pipe, Fig. 14(b) "Vedat", is found to give an accurate indication of the time taken for the initial warm-up phase of a recirculating system. With a flow of 0.6 g/s the water reaches 35 °C (75% of its final recirculating temperature rise) after about 1.5 h but this is followed by a second, more gradual phase and takes a further hour to rise to 39 °C. Raising the flow rate to 1 g/s reduces the warm-up time to ≈54 min as well as raising the steady-state temperature. For comparison, the "cooling" curves in Fig. 14(b) start with the pipe full of hot water after running the tap and show the gradual return to the recirculation steady state. The flow rate influences the steady state temperature but not the rate of cooling.

The need to avoid any risk of Legionnaires' Disease is a complicating factor. Rhoads [29] found that convection in hot water pipes that prevented them cooling to ambient temperature led to a 1.5 to 6-fold increase in bacterial concentration. A detailed analysis of the growth of *Legionella* bacteria is beyond the scope of this paper but any such system if unused for long periods would require a means of heating periodically to >60 °C to kill bacteria. This might be achieved by increasing the recirculation flow rate or raising the supply temperature e.g. by using a heating element with a timer.

7. Heat loss and pumping power

7.1. Comparison of recirculating and conventional system heat losses

The variation in time-mean heat loss rate for a pipe that cools after use, Fig. 3, indicates that the daily mean heat loss for a pipe section would depend on the usage history. If used so regularly that the pipe never cools (zero cooling period, Fig. 3) the heat loss rate from a single 15 mm pipe in a 75 mm sleeve would be 70.5 W, considering as before a 15 m length with $\Delta T = 40°C$.

A pair of 15 and 8 mm pipes with an optimal m = 0.1, n = 0.58 as Fig. 12 would after reaching a steady state lose 52 W with a 0.59 g/s recirculating flow: this is lower than the single pipe's 70.5 W simply because the temperature falls along the pipe to give 40 °C at the delivery point. Whilst in use, with uniform temperature throughout, the heat loss rate $L(h_{10} + h_{20})\Delta T$ would rise to 86.4 W.

The time constant with zero flow is 120 min for the single pipe system. To allow a simple comparison, two usage profiles will be considered: with 1 tap use per hour between 7 am and 11 pm, and with one every two hours.

For the hourly cycle, 1 h after each use the single pipe would have cooled from 60 to 44 °C, so a thermal store would not be essential and the comparison will be between the heating requirements of a "traditional" insulated pipe and a recirculation system. The mean single-pipe heat loss during the 1 h cooling period would be 56.3 W (Fig. 3).

It was assumed that a 0.6 g/s pumped recirculation system would run from 5 am (to allow a 2 h warm up) until 11 pm, after which the pipework would be allowed to cool overnight, and that the flow periods would be a small fraction of the total time such that the non-flow periods would provide an accurate heat loss prediction. Using the temperature curves from Fig. 14(b), the mean warm-up (2 hr) and cool-down (1 hr) heat loss rates are 28.6 and 71.9 W.

For the hourly cycle the daily mean heat loss rate would be 45 W for the single pipe and 27% higher (57 W) for the recirculating system. In a temperate climate, for much of the year these heat losses are likely to contribute to space heating rather than being wasted; conversely without any corresponding reduction in central heating use, the increased losses in a recirculating system (12 W) would equate to less than 1% of the median domestic gas use (Table 2). If the heat were provided by a heat pump with COP = 3, the additional electrical power for 12 W of heat could be provided by a PV panel area of just 0.23 m^2 under typical UK conditions. This is an acceptable expense to achieve the convenience of instant hot water regardless of the interval between withdrawals.

For intervals >83 min a 15 mm single pipe system in a 75 mm insulation sleeve would cool below 40 °C and instantaneous hot water delivery would necessitate either a recirculating system or local store as Fig. 2(b). For a cycle with a withdrawal every 2 h

Table 2
Distribution of annual mean gas consumption rates for UK houses [27].

	Q1	Median	Q3
Annual MWh	8	12	17
Mean rate (W)	913	1370	1940

between 7 am and 11 pm a single pipe would cool from 60 °C to 34.7 °C before each withdrawal, giving a weighted mean daily heat loss rate of 38 W from the pipe or a total of 48 W including an assumed 10 W heat loss from the thermal store. The cool water in the pipe would refill the local store after each discharge, meaning that this heat loss would have to be balanced by electrical heating within the store. The local store temperature would be set at 60 °C to prevent *Legionella*.

For comparison, the mean heat loss from a 0.6 g/s recirculating system with this 2-hour cycle (and preheating 5–7 am as above) would be 53 W and this would require an electrical input of ≈18 W if using a heat pump with COP = 3 to heat the water. As an alternative to an equally-convenient local store the recirculation system therefore saves approximately 30 W of electrical power.

These values are only indicative and would in practice depend on pipe length, usage cycle, insulation details temperatures and environment. The small difference between the conventional and recirculating configurations is not significant: a recirculation system could provide the convenience of warm water on demand without a significant increase in losses.

7.2. Pumping power requirements

Further simulations of sleeved recirculating systems producing $\frac{T_{IN}-T_{DEL}}{T_{IN}-T_{amb}} = 0.5$ for delivery lengths ranging from L = 5 to 30 m were well correlated by:

- $\dot{m} = k_1 L$
- $\Delta P = k_2 L^2$
- $\Delta H_{sy} = k_3 L^2$
- $W = k_4 L^3$

The coefficients are given in Table 3. The overall heat loss (including losses from the return pipe) is $\dot{Q}_{12} \approx 1.06\dot{m}c(T_{IN} - T_{DEL})$.

The maximum distance from tank to tap that could generate the required flow rate using a thermosyphon is shown in the last column of Table 3, assuming for simplicity a 1 m vertical separation of the flow and return ports on the hot water tank and a horizontal pipe run from the flow port on the tank. When using an 8 mm return pipe (6.8 mm bore) this corresponds to $\frac{L}{D} \cong 2100$; for larger diameters the maximum L/D ratio is higher.

The steady-state operation of a thermosyphon must satisfy $\oint \rho \boldsymbol{g}.d\boldsymbol{s} - \Delta P = 0$ where $d\boldsymbol{s}$ is a displacement vector element in the flow direction and the pressure drop ΔP is a function of the flow velocity. A thermosyphon will work best when the heat source is as far as possible below the heat sink: it might be possible with a ground-level heat store but not one up in a loft. The start of circulation following an initially isothermal state has not been considered: successful operation would require more detailed installation-specific design. Cases unsuitable for a thermosyphon would need a circulating pump. Peristaltic pumps can supply up to 1.5 g/s and might therefore be suitable for such a low flow rate.

The use of a recirculating system removes any preference for using small bore pipe to minimise the hot water arrival time, albeit with an increased heat loss rate if insulation diameters are unchanged. Compared to the 15 + 8 mm pipes, the larger diameter combination (22 mm flow, 10 mm return) has two advantages: it would provide a higher flow rate for a given supply pressure and could allow a thermosyphon to operate over a longer pipe run.

The increased diameters with 22/10 mm pipes instead of 15/8 would raise heat loss rates by 24% (75 mm sleeve diameter); to keep the heat loss unchanged the outer diameter would have to increase to 117 mm.

8. Conclusions

Experiments on houses with 3, 4 and 5 bedrooms showed that houses of this size typically have a hot water delivery delay in the range 17–46 s and up to 5 L of water may need to be discharged before the delivery temperature reaches 40 °C. The delay period may be computed approximately from the hot/cold interface velocity or in more detail using a novel Method of Lines numerical solution to the heat transfer equations.

Using a small-bore pipe to reduce the hot water arrival delay does not appear feasible due to installation conventions regarding flow velocity.

Local heat stores close to the delivery point could be an effective *retro*-fit option to provide hot water during this delivery delay period. Such stores could either use a compact high-power instantaneous heater or, if using existing wiring, a low power heater to maintain the temperature of a 7 L hot water store. The energy required by an instantaneous heater would roughly equate to the heat lost from the water cooling in the pipe after delivery, whereas a storage system would also need to offset heat losses from its tank.

New-build houses with access to the pipe runs during installation would be better served by a recirculation system. This allows all the heat to be produced using a heat pump and avoids the need for bulky electrical installations at each delivery point. Recirculation has previously been considered for commercial buildings but not hitherto on a domestic scale.

Several recirculation systems could share a common pump. The required flow rate could be as little as 0.6 cm^3/sec, requiring a pumping power <1 mW. If the system operated on a timer to reduce heat loss during out of use periods, a warm-up period of 2 h each morning would suffice. Hot water pipes are however typically within the habitable envelope and for much of the year any heat loss would simply offset the need for heating rather than contributing to additional carbon emissions. For return pipes with $\frac{L}{d} < 2100$ the pressure drop is low enough that a simple thermosyphon system with 1 m drop could be used instead of a pump to generate the recirculating flow.

Steady state simulations for 15 mm pipes with 75 mm diameter insulation subject to a 1-hour withdrawal cycle show the heat loss of a recirculating system would be approximately 27% higher than from the equivalent single pipe. This increase corresponds to less than 1% of the typical domestic gas usage and would for at least part of the year contribute to space heating rather than being wasted. For systems using a heat pump, the additional electrical power could be provided by 0.23 m^2 of solar panel.

For intervals between hot water withdrawals exceeding 83 min, an insulated pipe would cool down below 40 °C and the provision of instantaneous hot water would then demand either a recirculation system or a local thermal store at the point of use. Calculations over a 2-hour cycle for a 15 m pipe length show a local heat store solution would require a daily mean 48 W of electrical power to re-

Table 3
Correlation coefficients for recirculating systems with spacing $m = 0.1$. The wall thicknesses for the large and small pipe in each pair were 0.7 and 0.6 mm respectively.

Pipe pair OD (mm)	Optimum n	k_1 (kg/ms)	k_2 (N/m^4)	k_3 (m^{-1})	k_4 (W/m^3)	L(m) at $\Delta H = 1$ m
15 & 8	0.571	3.9×10^{-5}	0.48	0.0050	1.91×10^{-8}	14.1
22 & 10	0.603	5.0×10^{-5}	0.21	0.0022	1.09×10^{-8}	21.0

heat water that had cooled in the pipework. The recirculating alternative would lose 53 W of heat, but this would be obtained efficiently using a heat pump. The extra electrical power to the heat pump would be just 18 W i.e. 30 W less than required for the local store system.

The optimum position for a pair of pipes within a common sleeve has been identified. For 15 and 8 mm diameter pipes in a 75 mm sleeve, the 15 mm pipe would be 27 mm below the insulation surface and the 8 mm pipe would lie 20 mm below the surface, leaving 5 mm between the two pipes.

The unsteady conduction equations have been solved by a "Method of Lines" implementation using the Matlab solvers for systems of differential equations. Results for a sudden flow start in a uniform pipe are in good agreement with an analytical solution. The numerical scheme can model a pipe network with multiple diameters and the start-up period in a recirculating system.

The steady-state and transient models presented here have a number of advantages over alternative approaches. This system of linked equations is easily solved in general-purpose, widely available numerical packages such as Matlab without requiring access to 3D CFD software or more specialised multi-physics codes e.g. COMSOL®. When executed in Matlab it is particularly easy to perform multiple simulations over a range of geometric parameters to optimise the insulation distribution and flow rate and then to plot and compare these in a flexible manner.

The use of a 1D grid in the transient model simplifies the problem definition and avoids the user-intensive grid generation that is often required by CFD codes. Compared to a 1D analytical solution, the numerical method can model spatial variations in initial conditions, pipe size and heat transfer coefficients as well as pipe-to-pipe heat fluxes and time-variation of inlet temperature. These may find broader application beyond the immediate interest in domestic hot water.

Future research should provide practical demonstrations of both pumped and thermosyphon recirculation systems and verify the code against the resulting data. For pumped systems this would include demonstrating a suitably reliable low-flow pump for long term operation; for thermosyphon operation the model should be extended to include the effect of buoyancy forces on flow rate. Both forms should provide an automatic facility for routinely sterilising against *Legionella* infection.

Declaration of Competing Interest

The authors declare that they have no known competing financial interests or personal relationships that could have appeared to influence the work reported in this paper.

Acknowledgements

The authors are grateful to the Engineering and Physical Sciences Research Council (EPSRC) for funding this work as part of a collaborative programme between Warwick, Loughborough and Ulster universities, reference EP/N021304/1. Matlab data and code used for the figures in this paper are openly available from https://wrap.warwick.ac.uk/133558.

Appendix A. . Heat losses from two pipes sharing a common insulation sleeve

The most space-efficient way of implementing a circulation system to keep pipes warm, Fig. 8, would be for the flow and return pipe pair to share a common insulation sleeve. The return pipe can be smaller in diameter than the flow pipe because it only needs to carry a low flow rate to balance the heat losses rather than supplying a basin or bath tap.

Given that heat transfer between the flow and return pipes tends to increase the end-to-end temperature difference along the flow pipe, it might seem prudent for pipes in a common sleeve to be separated rather than in contact. This geometry was studied to assess whether the benefit of the additional insulation in the sleeve outweighed the pipe-to-pipe heat transfer effect.

In the absence of an analytic thermal conduction solution for this geometry a 2-D steady-state heat conduction analysis was performed using the Matlab PDE toolbox, Fig. A.1. 5000 elements were used; a grid refinement exercise at typical Biot numbers showed the heat flux changed by less than 0.05% relative to a solution with 20,000 elements.

For plotting purposes the geometry has been defined in terms of 4 non-dimensional parameters.

The pipe size fraction is defined as $f = \frac{r_1}{r_1+r_2}$ and the combined size ratio $g = \frac{r_1+r_2}{r_o}$, hence the pipe radii are $\{f, 1-f\} \times gr_o$.

Defining three gap dimensions as A (pipe 1 to insulation), B (pipe 2 to insulation) and C (central gap), the central gap fraction is $m = \frac{C}{A+B+C}$. The outer gap fraction is $n = \frac{A}{A+B}$; values of f, g, m and n in the range [0,1] avoid any overlap of the pipes. The pipe centre positions are $y_1 = (2(1-g)(1-m)n + fg - 1)r_0$ and $y_2 = (1 - 2(1-g)(1-m)(1-n) - (1-f)g)r_0$

For simplicity this analysis was done with constant pipe wall temperatures. This is justifiable because the pipe walls will have much higher conductivity than the insulation and impose a uniform wall temperature around each pipe. The external boundary condition was a circumferentially uniform heat transfer coefficient to simulate the effect of air convection.

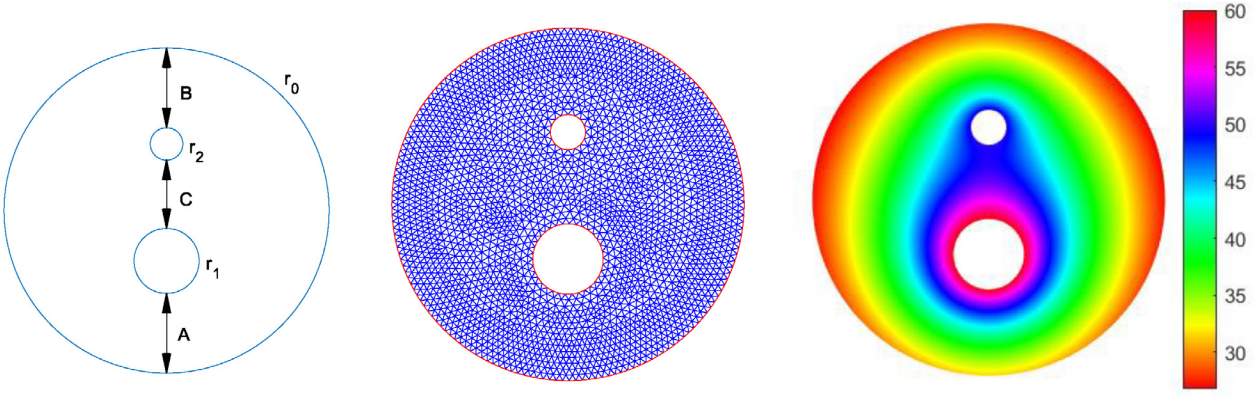

Fig. A1. Geometry definition with separated pipes, showing a typical temperature solution.

The PDE solution provides heat flux across the three surfaces Q_0, Q_1 and Q_2 (outer surface, pipe 1, pipe 2) for a vector of three temperatures T_0, T_1 and T_2. These three heat fluxes are not independent because $Q_0 = Q_1 + Q_2$: there are insufficient degrees of freed om for a single simulation to be decomposed into three heat transfer coefficients. By solving using two independent temperature vectors A, B the heat transfer coefficients (per m pipe length) h_{10}, h_{20} and h_{12} were obtained via a simultaneous equation:

$$\begin{bmatrix} \Delta \boldsymbol{T}_A \\ \Delta \boldsymbol{T}_B \end{bmatrix} \begin{bmatrix} h_{12} \\ h_{10} \\ h_{20} \end{bmatrix} = \begin{bmatrix} Q_0 \\ Q_1 \\ Q_2 \end{bmatrix} \text{ where } \Delta \boldsymbol{T_A} = \begin{bmatrix} 0 & \Delta T_{10A} & \Delta T_{20A} \\ \Delta T_{12A} & \Delta T_{10A} & 0 \\ -\Delta T_{12A} & 0 & \Delta T_{20A} \end{bmatrix}$$

and $\Delta T_{12} = T_1 - T_2$ etc.

The overall heat transfer coefficients including water-side heat transfer coefficients were then obtained by converting the above pi-network thermal resistance description into a T-network, adding thermal resistance to represent the water-side heat transfer coefficients and then converting back to a pi-definition.

The volume-weighted mean temperature was characterised as a linear function of the surface temperatures $\bar{T} = a_0 T_0 + a_1 T_1 + a_2 T_2$ such that $a_0 + a_1 + a_2 = 1$. As above, solutions A and B were used to obtain the coefficients by solving:

$$\begin{bmatrix} 1 & 1 & 1 \\ T_{0A} & T_{1A} & T_{2A} \\ T_{0B} & T_{1B} & T_{2B} \end{bmatrix} \begin{bmatrix} a_0 \\ a_1 \\ a_2 \end{bmatrix} = \begin{bmatrix} 1 \\ \bar{T}_A \\ \bar{T}_B \end{bmatrix}$$

References

[10] H. Averfalk, Pipe sizing for novel heat distribution, Energies 12 (7) (2019), https://doi.org/10.3390/en12071276 p1276.

[11] E. Bedard, *Legionella pneumophila* levels and sequence-type distribution in hospital hot water samples from faucets to connecting pipes, Water Research 156 (2019) 277–286.

[2] T. Benakopoulos, W. Vergo, M. Tunzi, R. Salenbien, S. Svendsen, Overview of Solutions for the Low-Temperature Operation of Domestic Hot-Water Systems with a Circulation Loop, Energies 14 (2021) 3350, https://doi.org/10.3390/en14113350.

[3] A. Bertrand, A. Mastrucci, N. Schüler, R. Aggoune, F. Maréchal, Characterisation of domestic hot water end-uses for integrated urban thermal energy assessment and optimisation, Applied Energy 186 (2017) 152–166, https://doi.org/10.1016/j.apenergy.2016.02.107.

[4] B. Bøhm, Production and distribution of domestic hot water in selected Danish apartment buildings and institutions. Analysis of consumption, energy efficiency and the significance for energy design requirements of buildings, Energy Conversion and Management 67 (2013) 152–159, https://doi.org/10.1016/j.enconman.2012.11.002.

[5] Bower, D. Keep it moving: Design strategies for maintaining water flow. PM Engineer, Vol.21, Iss. 9, (Sept 2015): 9-10. https://www.pmengineer.com/publications/3/editions/1288

[6] BRE Ltd, Hot Water Consumption, 2019 https://www.bregroup.com/heatpumpefficiency/hot-water-consumption (downloaded 5/2/2020).

[7] Chertkov, M. and Novitsky, N.N., Thermal Transients in District Heating Systems, Energy Volume 184, Oct 2019, pp22-33. https://arxiv.org/abs/1702.07634

[8] Eatherton. M., Challenges in DHW distribution -Part 1. Contractor Magazine. Dec2018, Vol. 63 Issue 12, p28-28. https://www.contractormag.com/management/eatherton/article/20883672/challenges-in-dhw-distribution-part-1

[9] Eatherton. M., Challenges in DHW distribution – Part 3. Contractor Magazine. Feb2019, Vol. 64 Issue 2, p26. https://www.contractormag.com/management/eatherton/article/20883765/challenges-in-dhw-distribution-part-3

[12] Freidt, K. Benefits of Hot Water Recirculation. Plumbing & Mechanical, Troy, Vol. 32, Iss. 3 (May 2014) 10-12.

[13] I. Gabrielaitiene, B. Bøhm, B. Sunden, Evaluation of Approaches for Modelling Temperature Wave Propagation in District Heating Pipelines, Heat Transfer Engineering 29 (1) (2008) 45–56, https://doi.org/10.1080/01457630701677130.

[14] R.H. Garrett (Ed.), Hot and Cold Water Supply, Blackwell Science Ltd, Oxford, UK, 2000.

[15] GASTEC, 2009, Final Report: In-situ monitoring of efficiencies of condensing boilers and use of secondary heating. https://assets.publishing.service.gov.uk/government/uploads/system/uploads/attachment_data/file/180950/In-situ_monitoring_of_condensing_boilers_final_report.pdf

[16] Gu, L, A Simplified Hot Water Distribution System Model. 10th International Building Performance Simulation Association Conference and Exhibition on September 3-6, 2007, Beijing, China http://fsec.ucf.edu/en/publications/pdf/FSEC-PF-429-07.pdf

[17] V.J. Haines, K. Kyriakopoulou, C. Lawton, End user engagement with domestic hot water heating systems: Design implications for future thermal storage technologies, Energy Research & Social Science 49 (March 2019) 74–81, https://doi.org/10.1016/j.erss.2018.10.009.

[18] A. Hamburg, A. Mikola, T.-M. Parts, T. Kalamees, Heat loss due to domestic hot water pipes, Energies 14 (2021) 6446, https://doi.org/10.3390/en14206446.

[19] Hamdi, S., Scheisser, W.E. and Griffiths, G.W. Method of Lines, Scholarpedia, 2 (7):2859, 10.4249/scholarpedia.2859

[20] Hansard, Spring Statement 2019, https://hansard.parliament.uk/commons/2019-03-13/debates/5B9C772E-1769-437A-A4F0-06DEAC55D676/SpringStatement

[21] O. Kaynakli, Economic thermal insulation thickness for pipes and ducts: A review study, Renewable and Sustainable Energy Reviews 30 (2014) 184–194, https://doi.org/10.1016/j.rser.2013.09.026.

[22] H. Kazmi, F. Mehmood, S. Lodeweyck, J. Driesen, Gigawatt-hour scale savings on a budget of zero: Deep reinforcement learning based optimal control of hot water systems, Energy 144 (2018) 159–168, https://doi.org/10.1016/j.energy.2017.12.019.

[23] T. Kitzberger, D. Kilian, J. Kotik, T. Pröll, Comprehensive analysis of the performance and intrinsic energy losses of centralized Domestic Hot Water (DHW) systems in commercial (educational) buildings, Energy & Buildings 195 (2019) 126–138, https://doi.org/10.1016/j.enbuild.2019.05.016.

[24] D. Marini, R.A. Buswell, C.J. Hopfe, Development of a dynamic analytical model for estimating waste heat from domestic hot water systems, Energy & Buildings 247 (2021), https://doi.org/10.1016/j.enbuild.2021.111119 111119.

[25] R.W. Moss, G.S.F. Shire, P. Henshall, P.C. Eames, F. Arya, and Hyde, T, Optimal passage size for solar collector microchannel and tube-on-plate absorbers, Solar Energy (2017), https://doi.org/10.1016/j.solener.2017.05.030.

[26] NREL, Domestic hot water system modelling for the design of energy efficient systems, 2002. www.homeinnovation.com/-/media/Files/Reports/domestichotwater.pdf

[27] OFGEM, Proposed updates to Typical Domestic Consumption Values (TDVCs), 2019, https://www.ofgem.gov.uk/system/files/docs/2019/10/tdcvs_2019_open_letter_0.pdf

[28] T. Oppelt, T. Urbaneck, U. Gross, B. Platzer, Dynamic thermo-hydraulic model of district cooling networks, Applied Thermal Engineering 102 (2016) 336–345, https://doi.org/10.1016/j.applthermaleng.2016.03.168.

[29] W. Rhoads, A. Pruden, M. Edwards, Convective Mixing in Distal Pipes Exacerbates Legionella pneumophila Growth in Hot Water Plumbing, Pathogens 5 (1) (2016) 29, https://doi.org/10.3390/pathogens5010029.

[30] L.F. Shampine, M.W. Reichelt, The MATLAB ODE Suite, SIAM Journal on Scientific Computing 18 (1) (1997) 1–22.

[31] L.F. Shampine, M.W. Reichelt, J.A. Kierzenka, Solving Index-1 DAEs in MATLAB and Simulink, SIAM Review 41 (3) (1999) 538–552.

[32] Sugden, The 2020s is the decade to decarbonise heat. Delta EE White Paper, https://www.delta-ee.com/index.php?option=com_edocman&view=document&id=2633

[33] B. van der Heijde, M. Fuchs, C.R. Tugorese, G. Schweiger, K. Sartor, D. Basciotti, D. Müller, C. Nytsch-Geusen, M. Wetter, L. Helsen, Dynamic equation-based thermo-hydraulic pipe model for district heating and cooling systems, Energy Conversion and Management 151 (2017) 158–169, https://doi.org/10.1016/j.enconman.2017.08.072.

[34] B. van der Heijde, A. Aertgeerts, L. Helsen, Modelling steady-state thermal behaviour of double thermal network pipes, International Journal of Thermal Sciences 117 (2017) 316–327, https://doi.org/10.1016/j.ijthermalsci.2017.03.026.

[35] K. Vanthournout, R. D'hulst, D. Geysen, G. Jacobs, A smart domestic hot water buffer, IEEE Transactions on Smart Grid 3 (4) (2012) 2121–2127, https://doi.org/10.1109/TSG.2012.2205591.

[36] S.A. Vedat, Conduction heat transfer, Addison-Wesley (New York), 1966, available from scribd.com.

[37] Wendt, R., Baskin, E. and Durfee, D. Evaluation of Residential Hot Water Distribution Systems by Numeric Simulation. Oak Ridge National Laboratory, 2004. http://www.ornl.gov/webworks/cppr/y2001/rpt/122464.pdf

[38] Wojtkowiak, J. Investigations of hot water temperature changes at the pipe outflow. E3S Web of Conferences 22, 00186 (2017) *ASEE17*, http://www.10.1051/e3sconf/20172200186